GEOPHYSICAL RESEARCH LETTERS, VOL. 22, NO. 11, PAGES 1377-1380, JUNE 1, 1995

On the utility of the molecular oxygen dayglow emissions as proxies for middle atmospheric ozone

Martin G. Mlynczak
NASA Langley Research Center, Hampton, Virginia

Daphne S. Olander[1]
Science Applications International Corporation, Hampton, Virginia

Abstract. The molecular oxygen dayglow emissions, $O_2(a^1\Delta_g \rightarrow X^3\Sigma_g)$ at 1.27 μm and $O_2(b^1\Sigma_g \rightarrow X^3\Sigma_g)$ at 762 nm, arise in part from processes related to the Hartley band photolysis of ozone. It is therefore possible to derive daytime ozone concentrations from measurements of the volume emission rate of either dayglow. The accuracy to which the ozone concentration can be inferred depends on the accuracy to which numerous kinetic and spectroscopic rate constants are known, including rates which describe the excitation of molecular oxygen by processes that are not related to the ozone concentration. We find that several key rate constants must be known to better than 7% accuracy in order to achieve an inferred ozone concentration accurate to 15% from measurements of either dayglow. Currently, accuracies for various parameters typically range from 5% to 100%.

Introduction

Understanding the distribution of ozone in the terrestrial mesosphere and lower thermosphere is a fundamental problem in atmospheric science. A complete description of the thermal structure and photochemistry of the region is not fully possible unless the ozone abundance is well characterized. To understand the distribution of ozone on a global basis requires remote detection from space-based observing platforms. The ozone concentration may be determined directly by measurements of emission from ozone itself and indirectly from measurements of emission from species that are produced as a result of ozone photolysis. Specifically, the two lowest-lying electronically excited states of molecular oxygen, $O_2(a^1\Delta_g)$ and $O_2(b^1\Sigma_g)$ (hereafter $O_2(^1\Delta)$ and $O_2(^1\Sigma)$) are created, in part, directly and indirectly as a result of photolysis in the Hartley band of ozone. Radiative emission from these two states thus provides an indirect measure of the ozone abundance. Observation of the $O_2(^1\Delta)$ airglow at 1.27 μm has been used to infer the ozone concentration by the Solar Mesosphere Explorer (SME) experiment [Thomas et al., 1984], and the $O_2(^1\Sigma)$ airglow at 762 nm as measured by the High-Resolution Doppler Imager (HRDI) on the Upper Atmosphere Research Satellite (UARS) is currently being considered as an ozone proxy [Yee et al., 1993]. The $O_2(^1\Delta)$ airglow will also be observed by the Sounding of the Atmosphere using Broadband Emission Radiometry (SABER) experiment [Russell et al., 1994] selected for NASA's Thermosphere-Ionosphere-Mesosphere Energetics and Dynamics (TIMED) mission.

The purpose of this letter is to identify the key kinetic and spectroscopic rates which relate the measured airglow intensities to the ozone concentration and to define quantitatively the accuracy to which these rates must be known in order to achieve an ozone concentration with an uncertainty of 15%, in order to guide new laboratory measurements. This study is similar to that of Harries [1982] who determined the rate constant accuracies required to achieve a good inference of hard-to-measure chemical species given measurements of related species and the photochemical relations between the species. We will show, using an approach similar to Harries', that significant improvements in the accuracy of the rate constants which describe collisional energy transfer, radiative absorption, and spontaneous emission in the coupled oxygen-ozone dayglow system are needed before ozone can be confidently inferred to an accuracy of 15% or better.

Methodology

The oxygen dayglow model used in this study is described by Mlynczak et al. [1993] and the relevant processes are listed in Table 1. The reader is referred to Figure 1 of Mlynczak et al. [1993] for a schematic illustration of the processes which generate molecular oxygen airglow. There are a total of 26 parameters which must be specified in order to calculate the $O_2(^1\Delta)$ or $O_2(^1\Sigma)$ volume emission rate. However, as will be shown, accurate inference of ozone from either dayglow requires good knowledge of 6 to 8 parameters.

To calculate the uncertainty in ozone due to uncertainties in the parameters, we evaluate the following expression for the standard deviation (variance) of the inferred ozone

$$S^2 = \sum_i \left[\frac{1}{O_3} \frac{\partial O_3}{\partial x_i} s_i \right]^2 \qquad (1)$$

where S^2 is the total variance (ultimately expressed as a percentage of the true ozone concentration), O_3 is the true ozone concentration, $\partial O_3/\partial x_i$ is the derivative of the ozone concentration with respect to kinetic or spectroscopic parameter x_i, and s_i is the uncertainty in parameter x_i. It is assumed that the individual parameters x_i are uncorrelated such that the total uncertainty S ($S = (S^2)^{1/2}$) in the inferred ozone concentration is given by the root-sum-square of the individual uncertainties, as in Harries [1982]. The terms composing the sum on the right hand side of Eq. 1 are evaluated numerically by first calculating the

[1]Now at NOAA Science Center, Washington, DC 20233.

Paper number 95GL01321

Table 1. Kinetic and spectroscopic processes in the molecular oxygen airglow.

Process	Rate Symbol	Description
$O_3 + h\nu \rightarrow O_2(^1\Delta) + O(^1D)$	$\phi_a J_a$	Hartley photolysis
$O_2 + h\nu \rightarrow O(^3P) + O(^1D)$	$\phi_L J_L$	Ly-α photolysis
$O_2 + h\nu \rightarrow O(^3P) + O(^1D)$	J_S	Schum.-Run. photol.
$O_2 + h\nu$ (762 nm) $\rightarrow O_2(^1\Sigma)$	J_{1S}	Solar absorption
$O(^1D) + N_2 \rightarrow O(^3P) + N_2$	k_c	Collisional quench.
$O(^1D) + O_2 \rightarrow O_2(^1\Sigma) + O(^3P)$	$\phi_d k_d$	Collisional quench.
$O(^1D) + O_2 \rightarrow O_2 + O(^3P)$	$(1-\phi_d)k_d$	
$O_2(^1\Delta) + O_2 \rightarrow O_2 + O_2$	k_i	Collisional quench.
$O_2(^1\Delta) + N_2 \rightarrow O_2 + N_2$	k_j	Collisional quench.
$O_2(^1\Delta) + O \rightarrow O_2 + O$	k_l	Collisional quench.
$O_2(^1\Delta) \rightarrow O_2 + h\nu$ (1.27 μm)	A_H	Spontan. emission
$O_2(^1\Sigma) + M \rightarrow O_2(^1\Delta) + M$	$\phi_e k_f$	Collisional quench.
$O_2(^1\Sigma) + M \rightarrow O_2(^3\Sigma) + M$	$(1-\phi_e k_f)$	
$O_2(^1\Sigma) \rightarrow O_2 + h\nu$ (762 nm)	A_K	Spontan. emission

molecular oxygen volume emission rate, then perturbing an individual parameter (such as a quenching rate), followed by deriving the ozone concentration using the calculated volume emission rate and the perturbed value of the specified parameter. This is done for each parameter as a function of height between 10 hPa (approximately 30 km) to 10^{-4} hPa (approximately 110 km). The model atmosphere is taken from Garcia and Solomon [1983, 1985] at equinox and low latitudes.

Results

As discussed by Mlynczak et al. [1993], $O_2(^1\Delta)$ can be generated directly upon photolysis of ozone in the Hartley band and indirectly by quenching of the $O_2(^1\Sigma)$ state. The $O_2(^1\Sigma)$ state can be generated in two different ways including direct excitation by sunlight at 762 nm and by energy transfer from $O(^1D)$. There are a total of five sources of $O_2(^1\Delta)$ and four sources of $O_2(^1\Sigma)$ considered in this work. Shown in Figures 1 and 2 are the relative contribution of each source to the total $O_2(^1\Delta)$ and $O_2(^1\Sigma)$ abundances, respectively. The sources corresponding to each numbered curve are described in the figure captions.

We apply the methodology described above to the problem of inferring the ozone concentration from measured oxygen airglow emission intensities initially assuming the following uncertainties in each parameter: 5% in A_K; 6% in ϕ_a, 10% in ϕ_e; 15% in J_{1S}, J_a, and A_H; 20% in J_S, J_L, k_c, k_d, k_f, k_i, k_j, and k_l; 30% in ϕ_d; and ϕ_L was varied between 0.44 and 1.0. Species densities (N_2, O_2, CO_2, O_3, and O) and temperature were held fixed in both forward and inverse calculations. Varying the quenching rates of $O_2(^1\Sigma)$ by O_2, CO_2, O_3, and O by 20% resulted in no significant uncertainty in retrieved ozone.

Shown in Table 2 are the results of the study for inferring ozone from measurements of $O_2(^1\Delta)$ emission. In each column is the percentage change (as a function of altitude) in the inferred ozone concentration due to the indicated change in the parameter listed at the top of each column. The six parameters listed (J_{1S}, J_a, A_H, ϕ_d, ϕ_e, and k_i) account for nearly all of the variance in the retrieved ozone. The column labeled RSS is the root-sum square of the error due to the uncertainties in all parameters. In this column we see that at the indicated levels of parameter uncertainty the inferred ozone is accurate from 25% to 30% below 80 km and from 17% to 20% between 80 and 90 km. Above 90 km the uncertainty rapidly increases because ozone provides only a small fraction of the $O_2(^1\Delta)$ abundance. The stated goal of 15% uncertainty is not achieved with uncertainties of 10% to 30% in the six key parameters listed in Table 2. The total systematic error presented here for ozone concentrations derived from measurements of $O_2(^1\Delta)$ emission are consistent with those presented for the SME experiment by Thomas et al. [1984].

An important question is by how much should the uncertainties be reduced in order to bring the total uncertainty in retrieved ozone below 15%. For simplicity, we require that each of the six parameters be known to the same accuracy and then determine the minimum uncertainty required to bring the overall uncertainty in the inferred ozone below 15% over most of the altitude range.

The column labeled RSS' in Table 2 is the total uncertainty in inferred ozone calculated using a 7% uncertainty in the six key parameters identified above. The uncertainties in all other parameters are unchanged. Below ~92 km the accuracy is better than 15% except near 75 km where the uncertainty approaches 20%. As shown in Figure 1, above 92 km and near 75 km, ozone is responsible for less than half of the $O_2(^1\Delta)$, and the inferred ozone at these altitudes is very sensitive to relatively small uncertainties in the airglow model parameters. From this analysis we conclude that the six key rate constants defined above need to be known to an accuracy of about 7% or better to allow ozone to be inferred from measurements of the $O_2(^1\Delta)$ airglow to an accuracy of 15%. Of the six parameters, J_{1S} and J_a are not laboratory measured rates but are calculated using solar intensity, absorption cross section, and atmospheric composition data. As such, future laboratory research should concentrate on improvements in parameters A_H, ϕ_d, ϕ_e, and k_i. Priority should

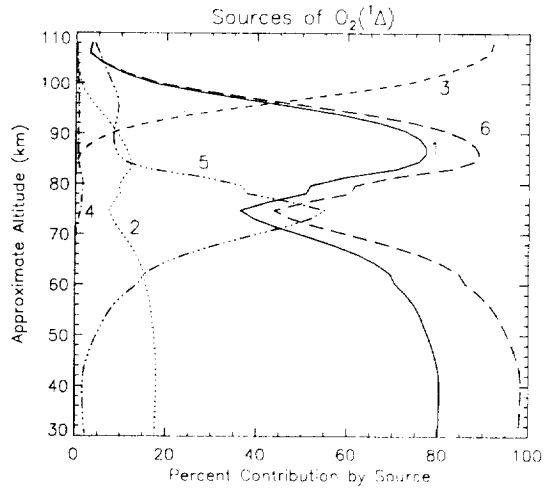

Figure 1. Relative magnitude of sources of $O_2(^1\Delta)$. Curve 1 is production directly from ozone photolysis. Curves 2 through 5 represent production of $O_2(^1\Delta)$ from collisional quenching of $O_2(^1\Sigma)$. Curve 2 is production indirectly from $O(^1D)$ generated by ozone photolysis, Curve 3 is production indirectly from $O(^1D)$ generated by O_2 photolysis in the Schumann-Runge continuum, Curve 4 is production indirectly from O_2 photolysis at Ly-α wavelengths, and Curve 5 is from production of $O_2(^1\Sigma)$ by absorption of sunlight at 762 nm. Curve 6 is the sum of Curves 1 and 2 which represents the total ozone-related production of $O_2(^1\Delta)$.

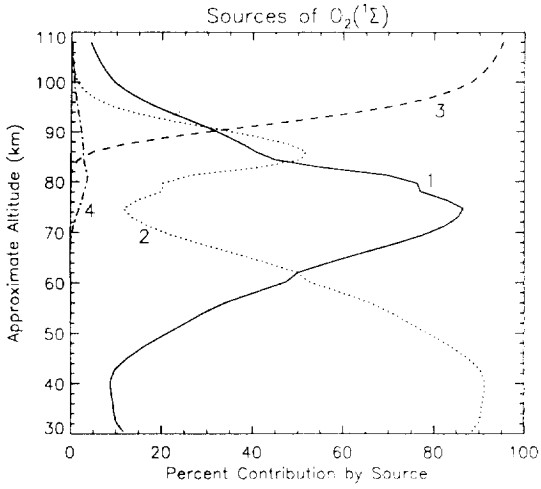

Figure 2. Relative magnitudes of sources of $O_2(^1\Sigma)$. Curve 1 is production due to resonant absorption of sunlight at 762 nm, Curve 2 production due to energy transfer from $O(^1D)$ generated directly from ozone photolysis, Curve 3 is production due to $O(^1D)$ generated by photolysis of O_2 in the Schumann-Runge continuum, and Curve 4 is production due to $O(^1D)$ generated by photolysis of O_2 at Ly-α wavelengths.

be placed upon A_H and k_i as the root-sum-square of the errors due to uncertainty in ϕ_d and ϕ_e below ~92 km is small (6%-7%) except near 75 km.

In a similar manner the uncertainty in inferred ozone from measurements of the $O_2(^1\Sigma)$ airglow was determined. The results are listed in Table 3 in the same fashion as Table 2. Initial parameter uncertainties are as given above for the $O_2(^1\Delta)$ airglow. We find that eight parameters (J_{1S}, J_a, A_K, ϕ_d, ϕ_L, k_c, k_d, and k_f) contribute most to the variance, and at the stated initial levels of parameter uncertainty the accuracy in inferred ozone is no better than 50% (column RSS) at all altitudes. The uncertainty is very large near 75 km and above 90 km because ozone is responsible for less than half of the $O_2(^1\Sigma)$ at those altitudes (as shown in Figure 2).

Because of the large uncertainty in $O_2(^1\Sigma)$-inferred ozone at all altitudes, we specified a 5% uncertainty on all parameters and then recalculated the uncertainty in inferred ozone, which is given in the column labeled RSS' in Table 3. The goal of 15% is achieved only below 60 km and near 85 km where, as shown in Figure 2, ozone is responsible for more than half of the $O_2(^1\Sigma)$. Between 60 and 85 km, processes involving ozone generate only 10% to 50% of the $O_2(^1\Sigma)$, and the inferred ozone is therefore extremely sensitive to parameter uncertainty.

From this analysis, it appears that the $O_2(^1\Sigma)$ dayglow may provide a good proxy for ozone in the upper stratosphere and lower mesosphere (30 to 60 km) and also near 85 km. However, as with the $O_2(^1\Delta)$ airglow, there needs to be significant improvement in the knowledge of kinetic and spectroscopic rates. Specifically, below 60 km there are six parameters whose uncertainty is responsible for virtually all of the uncertainty in the inferred ozone, J_a, k_c, k_d, ϕ_d, k_f, and A_K. Of these six parameters, J_a and ϕ_d are also indicated for improvement above in the discussion of the $O_2(^1\Delta)$ airglow. It is unlikely that the accuracy of A_K (5%) will be improved, so future laboratory research should focus on improving k_c, k_d, and k_f to an accuracy of ~5%.

There are other sources of systematic error to be considered other than rate constant uncertainty. These may include instrument calibration errors, radiative transfer errors, line-of sight O_2 abundance errors, instrument pointing, and temperature-pressure registration. Typical uncertainties (< 3 K) in simultaneously measured temperatures will not cause additional significant error in the rate constants provided the temperature dependence is known over the range of expected temperatures (140 K to 270 K). Of these additional error mechanisms, instrument calibration can be a serious error component of upper mesospheric and lower thermospheric ozone inferred from measurements of $O_2(^1\Sigma)$ even if the kinetics are well known. Shown in Tables 2 and 3 in the columns labeled Cal is the error in inferred ozone due to a 5% uncertainty in the absolute calibration of an instrument which determines the $O_2(^1\Delta)$ or $O_2(^1\Sigma)$ volume emission rate. Calibration errors result in large uncertainties (10% to 100%) in $O_2(^1\Sigma)$-inferred ozone above 60 km because ozone is responsible for a small portion of the total $O_2(^1\Sigma)$ abundance.

Finally, we have also considered the impact that simultaneous measurements of both oxygen airglows would have on the uncertainty in the derived ozone concentration. $O_2(^1\Sigma)$-derived ozone is independent of the $O_2(^1\Delta)$ concentration, but $O_2(^1\Delta)$-derived ozone is not. Therefore, simultaneous measurements of both airglows could possibly reduce the uncertainty only in $O_2(^1\Delta)$-derived ozone. However, our studies show that if the $O_2(^1\Sigma)$ concentration is known (by measurement or calculation) to 10% accuracy there will be little improvement in the uncertainty in ozone concentrations derived from measurements of the $O_2(^1\Delta)$ airglow. This result is a consequence of the fact that the bulk of the uncertainty in $O_2(^1\Delta)$-derived ozone is from parameters such as J_a, A_H, and k_i which relate the $O_2(^1\Delta)$ emission rate to the ozone concentration and from the fact that (below ~92 km) the bulk of the $O_2(^1\Delta)$ is generated from ozone photolysis.

Table 2. Errors in retrieved ozone due to errors in kinetic and spectroscopic rate parameters associated with the $O_2(^1\Delta)$ airglow at 1.27 μm. See text for description.

Param. Error	J_{1S} 1.15	J_a 1.15	A_H 1.15	ϕ_d 1.3	ϕ_e 1.1	k_i 1.2	RSS	RSS'	Cal. 1.05
Z(km)									
100.0	-6.5	-13.0	-12.3	138.2	49.8	-0.5	236.3	190.3	29.4
96.9	-3.5	-13.0	-6.3	45.9	17.4	-0.4	74.2	56.5	13.2
93.7	-2.1	-13.0	-4.1	17.1	7.0	-0.5	30.6	22.2	8.0
90.6	-1.6	-13.0	-3.1	8.1	3.7	-0.7	20.6	14.9	6.3
87.5	-1.5	-13.0	-2.6	5.3	2.7	-1.2	17.8	12.3	5.7
84.4	-1.9	-13.0	-2.4	4.8	2.8	-2.1	16.8	10.8	5.7
81.3	-6.0	-13.0	-3.4	5.5	5.9	-4.6	19.2	11.8	7.1
78.1	-9.3	-13.0	-5.8	5.9	8.2	-8.5	23.1	13.5	8.2
74.7	-18.9	-13.0	-11.8	6.3	14.8	-17.5	36.2	19.5	11.5
71.3	-12.7	-13.0	-13.0	5.8	10.5	-19.3	32.7	16.6	9.3
67.8	-6.6	-13.0	-12.7	5.6	6.3	-18.9	29.2	14.4	7.2
64.1	-3.6	-13.0	-12.7	5.7	4.2	-18.9	28.3	13.8	6.2
60.2	-2.4	-13.0	-13.1	5.7	3.5	-19.6	28.8	13.9	5.8
56.1	-1.4	-13.0	-13.1	5.8	2.8	-19.6	28.7	13.8	5.5
51.7	-0.9	-13.0	-13.2	5.8	2.5	-19.7	28.7	13.8	5.3
47.3	-0.5	-13.0	-13.1	5.8	2.2	-19.7	28.6	13.8	5.2
42.8	-0.3	-13.0	-13.1	5.8	2.1	-19.6	28.6	13.7	5.1
38.5	-0.3	-13.0	-13.2	5.8	2.0	-19.7	28.6	13.7	5.1
34.4	-0.3	-13.0	-13.2	5.8	2.0	-19.8	28.7	13.8	5.1
30.5	-0.4	-13.0	-13.3	5.7	2.1	-19.9	28.8	13.8	5.1

Table 3. Errors in retrieved ozone due to errors in kinetic and spectroscopic rates associated with the $O_2(^1\Sigma)$ airglow at 762 nm. See text for description.

Parameter: Uncertainty:	J_{1S} 1.15	J_a 1.15	A_K 1.05	ϕ_d 1.3	ϕ_L 2.24	k_c 1.2	k_d 1.20	k_f 1.20	RSS	RSS'	Cal. 1.05
Z(km)											
100.0	-101.0	-13.0	-129.0	3012.0	-61.0	-1056.0	1320.0	139.0	3811.2	954.8	387.5
96.9	-44.0	-13.0	-44.0	809.0	-27.0	-280.0	350.0	65.0	1017.2	250.0	109.7
93.7	-22.0	-13.0	-17.0	252.0	-14.0	-86.0	108.0	35.0	312.5	72.6	37.3
90.6	-14.0	-13.0	-9.0	102.0	-8.0	-35.0	43.0	24.0	124.7	25.9	16.9
87.5	-11.0	-13.0	-6.0	58.0	-7.0	-20.0	25.0	22.0	73.1	14.9	10.9
84.4	-13.0	-13.0	-7.0	47.0	-7.0	-16.0	20.0	25.0	62.9	14.1	10.0
81.3	-39.0	-13.0	-15.0	48.0	-18.0	-16.0	20.0	57.0	92.2	26.5	18.9
78.1	-57.0	-13.0	-21.0	49.0	-20.0	-16.0	20.0	81.0	118.2	36.2	24.9
74.7	-111.0	-13.0	-38.0	50.0	-23.0	-17.0	21.0	147.0	198.8	65.0	43.1
71.3	-73.0	-13.0	-27.0	44.0	-6.0	-15.0	18.0	104.0	140.2	45.5	29.6
67.8	-37.0	-13.0	-16.0	42.0	0.0	-14.0	17.0	62.0	89.1	26.6	17.6
64.1	-19.0	-13.0	-10.0	42.0	0.0	-14.0	17.0	41.0	67.8	17.9	11.7
60.2	-13.0	-13.0	-8.0	42.0	0.0	-14.0	17.0	34.0	62.0	15.1	9.5
56.1	-7.0	-13.0	-7.0	42.0	0.0	-14.0	17.0	27.0	57.2	13.1	7.6
51.7	-4.0	-13.0	-6.0	42.0	0.0	-14.0	17.0	23.0	55.0	12.1	6.6
47.3	-2.0	-13.0	-5.0	42.0	0.0	-14.0	17.0	21.0	54.0	11.6	6.0
42.8	-1.0	-13.0	-5.0	42.0	0.0	-14.0	17.0	19.0	53.2	11.2	5.5
38.5	-1.0	-13.0	-5.0	42.0	0.0	-14.0	17.0	18.0	52.9	11.2	5.5
34.4	-1.0	-13.0	-5.0	42.0	0.0	-14.0	17.0	18.0	52.9	11.2	5.5
30.5	-1.0	-13.0	-5.0	42.0	0.0	-14.0	17.0	18.0	52.9	11.2	5.6

Discussion

It is evident from the results presented above that the molecular oxygen dayglows, $O_2(^1\Delta)$ and $O_2(^1\Sigma)$, may provide very accurate measures of the ozone concentration from the upper stratosphere into the lower thermosphere (below 92 km) if several key kinetic and spectroscopic parameters can be determined to accuracies of 5% to 7%, and if measurements are made with well-calibrated instruments. However, the uncertainties in most rates are far greater than 5% to 7%. In fact, the total uncertainties presented in the columns labeled RSS in Tables 2 and 3 may be optimistic. For example, at mesospheric temperatures, quenching rates k_c, k_d, k_i, and k_f are uncertain by 25% to 40% [JPL-92], while ϕ_e is uncertain by as much as 20% [Knickelbein et al., 1987]. In addition, a key parameter in the inference of ozone concentration from measurements of $O_2(^1\Delta)$ emission is the Einstein A-coefficient for spontaneous emission of the $O_2(^1\Delta)$ state, and it is uncertain by nearly a factor of 2, as shown by Mlynczak and Nesbitt [1995]. Finally, based on the results in the RSS' columns of Tables 2 and 3, it is unlikely that either oxygen airglow feature can provide an accurate (RSS < 15%) measure of the ozone concentration above ~92 km.

It is important that the kinetic and spectroscopic rates and mechanisms defined in this letter be better determined in the near future. A coordinated and focused laboratory effort is needed to determine the rate constants to the accuracies as described above. These efforts will greatly aid the study of mesospheric ozone through the potential reprocessing of SME data, the analysis of HRDI data, and the interpretation of new measurements from the SABER instrument.

References

Garcia, R. R., and S. Solomon, A numerical model of the zonally averaged dynamical and chemical structure of the middle atmosphere, *J. Geophys. Res.*, 88, 1379-1400, 1983.

Garcia, R. R., and S. Solomon, The effect of breaking gravity waves on the dynamics and chemical composition of the mesosphere and lower thermosphere, *J. Geophys. Res.*, 90, 3850-3868, 1985.

Harries, J. E., Stratospheric composition measurements as tests of photochemical theory, *J. Atm. Terr. Phys.*, 44, 591-597, 1982.

JPL, Jet Propulsion Laboratory, *Chemical kinetics and photochemical data for use in stratospheric modeling, JPL 92-20, Evaluation 10*, 196 pp., NASA Panel for Data Evaluation, Jet Propulsion Laboratory, Pasadena, Calif., 1992.

Knickelbein, M. B., K. L. Marsh, O. E. Ulrich, and G. E. Busch, Energy transfer kinetics of singlet molecular oxygen: The deactivation channel for $O_2(b^1\Sigma_g)$, *J. Chem. Phys.*, *87*, 2392-2393, 1987.

Mlynczak, M. G., and D. J. Nesbitt, The Einstein coefficient for spontaneous emission of the $O_2(a^1\Delta_g)$ state, *Geophys. Res. Lett.*, 22, 1995, in press.

Mlynczak, M. G., S. Solomon, and D. S. Zaras, An updated model for $O_2(a^1\Delta_g)$ concentrations in the mesosphere and lower thermosphere and implications for remote sensing of ozone at 1.27 μm, *J. Geophys. Res.*, 98, 18,639-18,648, 1993.

Russell, J. M. III, M. G. Mlynczak, and L.L. Gordley, An overview of the SABER experiment for the TIMED Mission, SPIE Proceedings 2266 Optical Spectroscopic Techniques and Instrumentation for Atmospheric and Space Research, Jinxue Wang and Paul B. Hays, Eds., 406-414, 1994.

Thomas, R. J., C. A. Barth, D. W. Rusch, and R. W. Sanders, Solar Mesosphere Explorer near-infrared spectrometer: Measurements of 1.27-μm radiances and the inference of mesospheric ozone, *J. Geophys. Res.*, 89, 9569-9580, 1984.

Yee, J. H., D. E. Anderson, C. I. Meng, R. DeMajistre, W. Sharp, W. Skinner, and P. B. Hays, Retrieval of $O(^1D)$ and O_3 number densities from measurements of the $O_2(^1\Sigma)$ atmospheric band, *Trans. Amer. Geophys. Union*, 74, 473, 1993.

Martin G. Mlynczak, NASA Langley Research Center, Mail Stop 401B, Hampton, VA 23681-0001

Daphne S. Olander, NOAA Science Center, E/RA21, 5200 Auth Road, Room 601, Washington, DC 20233.

(Received January 20, 1995; revised March 17, 1995; accepted March 28, 1995.)